Journal of Coastal Research	SI	62	30–39	West Palm Beach, Florida	Spring 2011

Post-Katrina Land-Cover, Elevation, and Volume Change Assessment along the South Shore of Lake Pontchartrain, Louisiana, U.S.A.

Molly K. Reif[†], Christopher L. Macon[‡], and Jennifer M. Wozencraft[§]

[†]U.S. Army Corps of Engineers
Engineer Research and Development Center, Environmental Laboratory
Joint Airborne LIDAR Bathymetry Technical Center of eXpertise
7225 Stennis Airport Road, Suite 100
Kiln, MS 39556, U.S.A.
Molly.k.Reif@usace.army.mil

[‡]U.S. Army Corps of Engineers
Mobile District
Joint Airborne LIDAR Bathymetry Technical Center of eXpertise
7225 Stennis Airport Road, Suite 100
Kiln, MS 39556, U.S.A.

[§]U.S. Army Corps of Engineers
Engineer Research and Development Center, Coastal and Hydraulics Laboratory
Joint Airborne LIDAR Bathymetry Technical Center of eXpertise
7225 Stennis Airport Road, Suite 100
Kiln, MS 39556, U.S.A.

www.cerf-jcr.org

ABSTRACT

REIF, M.K.; MACON, C.L., and WOZENCRAFT, J.M., 2011. Post-Katrina land-cover, elevation, and volume change assessment along the south shore of Lake Pontchartrain, Louisiana, U.S.A. *In:* Pe'eri, S. and Long, B. (eds.), *Applied LIDAR Techniques*, Journal of Coastal Research, Special Issue No. 62, 30–39. West Palm Beach (Florida), ISSN 0749-0208.

Advances in remote-sensing technology have led to its increased use for posthurricane disaster response and assessment; however, the use of the technology is underutilized in the recovery phase of the disaster management cycle. This study illustrates an example of a postdisaster recovery assessment by detecting coastal land cover, elevation, and volume changes using 3 years of post-Katrina hyperspectral and light detection and ranging data collected along the south shore of Lake Pontchartrain, Louisiana. Digital elevation models and basic land-cover classifications were generated for a 34-km^2 study area for 2005, 2006, and 2007. A change detection method was used to assess postdisaster land-cover, elevation, and volume changes. Results showed that the vegetation classes had area increases, whereas bare ground/roads and structures classes had area decreases. Overall estimated volume changes included a net volume decrease of 1.6 $\times$ 10^6 m^3 in 2005 to 2006 and a net volume decrease of 2.1 $\times$ 10^6 m^3 in 2006 to 2007 within the study area. More specifically, low vegetation and bare ground/roads classes had net volume increases, whereas medium and tall vegetation and structures classes had net volume decreases. These changes in land cover, elevation, and volume illustrate some of the major physical impacts of the disaster and ensuing recovery. This study demonstrates an innovative image fusion approach to assess physical changes and postdisaster recovery in a residential, coastal environment.

ADDITIONAL INDEX WORDS: *Hurricane Katrina, LIDAR, topography, land cover, recovery, change detection, Lake Pontchartrain, New Orleans, Joint Airborne LIDAR Bathymetry Technical Center of Expertise.*

INTRODUCTION

Advances in remote-sensing technology have led to its increased use for posthurricane disaster response and assessment. Many government agencies conduct surveys for postdisaster response and at no time was this more evident than after hurricane Katrina, in which more than 21 different platforms acquired various types of digital imagery in the days and weeks after the disaster (Womble *et al.*, 2006). Hurricane Katrina hit the northern gulf coast on August 29, 2005, causing widespread damage and loss of life, resulting in one of the most catastrophic natural disasters in U.S. history (Knabb, Rhome, and Brown, 2005). Many of the various rapid response surveys, including airborne and space-borne platforms, focused on assessing initial damage and loss caused by wind, flood, and storm surge. These included assessments of storm damage to buildings and other structural elements, detecting debris fields and affected nearshore features, and identifying flood and storm-surge extents and related damages (Barnes, Fritz, and Yoo, 2007; Friedland, Levitan, and Adams, 2008; Fritz *et al.*, 2007; Ghosh *et al.*, 2007; Hansen *et al.*, 2007; Stoker *et al.*, 2009; Vijayaraj, Bright, and Bhaduri, 2008; Womble *et al.*, 2006; Womble, Mehta, and Adams, 2008). Other assessments included vegetation- and forest-damage studies (FIA, 2005; Oswalt and Oswalt, 2008; Rodgers, Murrah, and Cooke, 2009; Wang and Xu, 2009; Wang *et al.*, 2010), as well as shoreline-change and beach-erosion studies, such as those prepared by Fearnley *et al.* (2009) and Froede (2008). Other regional assessments focused on land-area changes, specifically examining impacts to wetlands (Barras, 2006, 2007, 2009) and large-scale changes in land cover, such as in the Katrina Land Cover Change Data, 2005–2006, developed by the Coastal Change Analysis Program at the National Oceanic and Atmospheric Administration (NOAA) Coastal Services Center (NOAA, 2006).

Although there are many examples for the use of remote

DOI:10.2112/SI_62_4 received and accepted in revision 13 September 2010.
© Coastal Education & Research Foundation 2011

Report Documentation Page

Form Approved
OMB No. 0704-0188

Public reporting burden for the collection of information is estimated to average 1 hour per response, including the time for reviewing instructions, searching existing data sources, gathering and maintaining the data needed, and completing and reviewing the collection of information. Send comments regarding this burden estimate or any other aspect of this collection of information, including suggestions for reducing this burden, to Washington Headquarters Services, Directorate for Information Operations and Reports, 1215 Jefferson Davis Highway, Suite 1204, Arlington VA 22202-4302. Respondents should be aware that notwithstanding any other provision of law, no person shall be subject to a penalty for failing to comply with a collection of information if it does not display a currently valid OMB control number.

1. REPORT DATE	2. REPORT TYPE	3. DATES COVERED
2011		**00-00-2011 to 00-00-2011**

4. TITLE AND SUBTITLE
Post-Katrina Land-Cover, Elevation, and Volume Change Assessment along the South Shore of Lake Pontchartrain, Louisiana, U.S.A.

5a. CONTRACT NUMBER
5b. GRANT NUMBER
5c. PROGRAM ELEMENT NUMBER

6. AUTHOR(S)

5d. PROJECT NUMBER
5e. TASK NUMBER
5f. WORK UNIT NUMBER

7. PERFORMING ORGANIZATION NAME(S) AND ADDRESS(ES)
U.S. Army Corps of Engineers,Engineer Research and Development Center, Environmental Laboratory,7225 Stennis Airport Road, Suite 100, Kiln,MS, 39556

8. PERFORMING ORGANIZATION REPORT NUMBER

9. SPONSORING/MONITORING AGENCY NAME(S) AND ADDRESS(ES)

10. SPONSOR/MONITOR'S ACRONYM(S)
11. SPONSOR/MONITOR'S REPORT NUMBER(S)

12. DISTRIBUTION/AVAILABILITY STATEMENT
Approved for public release; distribution unlimited

13. SUPPLEMENTARY NOTES
Journal of Coastal Research, Special Issue No. 62, 2011

14. ABSTRACT

Advances in remote-sensing technology have led to its increased use for posthurricane disaster response and assessment; however, the use of the technology is underutilized in the recovery phase of the disaster management cycle. This study illustrates an example of a postdisaster recovery assessment by detecting coastal land cover, elevation, and volume changes using 3 years of post-Katrina hyperspectral and light detection and ranging data collected along the south shore of Lake Pontchartrain, Louisiana. Digital elevation models and basic land-cover classifications were generated for a 34- km2 study area for 2005, 2006, and 2007. A change detection method was used to assess postdisaster land-cover,elevation, and volume changes. Results showed that the vegetation classes had area increases, whereas bare ground/roads and structures classes had area decreases. Overall estimated volume changes included a net volume decrease of 1.6 3 106 m3 in 2005 to 2006 and a net volume decrease of 2.1 3 106 m3 in 2006 to 2007 within the study area. More specifically, low vegetation and bare ground/roads classes had net volume increases, whereas medium and tall vegetation and structures classes had net volume decreases. These changes in land cover, elevation, and volume illustrate some of the major physical impacts of the disaster and ensuing recovery. This study demonstrates an innovative image fusion approach to assess physical changes and postdisaster recovery in a residential, coastal environment.

15. SUBJECT TERMS

16. SECURITY CLASSIFICATION OF:			17. LIMITATION OF ABSTRACT	18. NUMBER OF PAGES	19a. NAME OF RESPONSIBLE PERSON
a. REPORT	b. ABSTRACT	c. THIS PAGE			
unclassified	**unclassified**	**unclassified**	**Same as Report (SAR)**	**11**	

sensing in posthurricane rapid response, some have noted that the technology is underutilized in the recovery phase of the disaster management cycle (Hill *et al.*, 2006; Ward, Leitner, and Pine, 2010). This means extending geographic study past the immediacy of the event into the recovery phase, which can take years, if not decades. It also means utilizing newer remote-sensing technologies that can provide improved or innovative capabilities for studying physical changes to coastal environments caused by events such as hurricanes. Two of these newer remote-sensing technologies that are proving useful for assessing coastal environments include light detection and ranging (LIDAR) elevation data and hyperspectral imagery (Chust *et al.*, 2008; Elaksher, 2008; Klemas, 2009).

LIDAR Data

LIDAR is a rapidly evolving remote-sensing technology that actively measures elevation. It emits light pulses and measures their time of flight between the sensor and target to determine the elevation of the ground surface, as well as other surface features (Lefsky *et al.*, 2002; NOAA, 2008). Data collection results in a dense cloud of elevation points that are used to generate digital elevation models (DEMs), illustrating a continuous representation of the earth's surface (NOAA, 2008). Each laser pulse is intercepted by objects on the earth's surface, providing a three-dimensional view of surface features, such as vegetation or structures. Most commercial topographic LIDAR systems are discrete return systems where single range measurements (returns) are recorded when the returned energy exceeds the manufacturer's threshold. Many of these systems record multiple returns for each emitted laser pulse. The return number refers to the order in which the laser pulse is returned, whereas the number of returns varies according to sensor model. The first return measures the height of the first object in the laser pulse flight path, whereas later returns (second, third, and ultimately the last return) measure the height of objects encountered midway to the ground or of the ground itself (Lefsky *et al.*, 2002).

Hyperspectral Data

Hyperspectral imaging is another rapidly growing remote-sensing technology. In general, these sensors collect imagery in many narrow, contiguous spectral bands in the electromagnetic spectrum (Lillesand, Kiefer, and Chipman, 2008). They can collect more than 200 bands of data and measure the spectral reflectance of objects on the earth's surface. Because of the narrow bandwidth, they are especially useful for characterizing objects that cannot be discerned with coarser bandwidths of more common multispectral remote sensors (Lillesand, Kiefer, and Chipman, 2008). Many of the sensors are programmable, such as the Compact Airborne Spectrographic Imager (CASI)-1500, which is a pushbroom hyperspectral sensor featuring up to 288 bands (375 to 1050 nm) at 1.9-nm intervals. Generally, the collected imagery is analyzed to identify features on the earth's surface on the basis of their spectral properties or spectral signatures. Hyperspectral remote sensing has many applications, ranging from surface mineralogy to bathymetry, and more recent analysis combining hyperspectral imagery with other data types, such as LIDAR, is providing new analytical methods for improved classification results (Geerling *et al.*, 2007; Hill and Thompson, 2005; Mundt, Streutker, and Glenn, 2006; Smith, Irish, and Smith, 2000; Wozencraft, Macon, and Lillycrop, 2007).

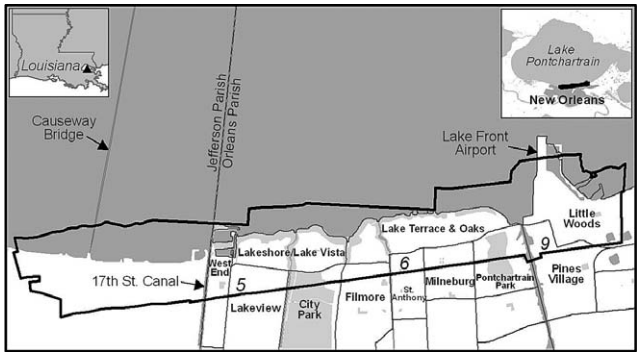

Figure 1. The study area, outlined in black, is 34 km^2 along the south shore of Lake Pontchartrain, Louisiana, including all or part of 11 neighborhoods and 3 districts (5, 6, and 9).

This study proposes to illustrate an example of a post-disaster recovery assessment by detecting coastal land-cover, elevation, and volume changes using 3 years (2005–2007) of post-Katrina hyperspectral and LIDAR data collected along the south shore of Lake Pontchartrain, Louisiana. The goals of this study are to (1) utilize imagery collected by a unique, integrated sensor suite ideally suited for image fusion, and (2) demonstrate how these remote-sensing techniques can be applied to assess physical changes and recovery of a residential, coastal environment in response to a hurricane.

METHODS

Study Area

The south shore of Lake Pontchartrain was chosen as a suitable area of analysis because of available data in the years after the disaster and because it is a representative residential, coastal area with varying population densities, socioeconomic conditions, and rates of recovery. More specifically, the region of analysis includes the area approximately 4 km W of the Lake Pontchartrain Causeway Bridge to approximately 2 km E of the New Orleans Lake Front Airport, which is nearly 34 km^2 (Figure 1). This area falls within both Jefferson and Orleans parishes and includes parts of 3 planning districts and 11 neighborhoods in Orleans Parish as defined by the New Orleans City Planning Commission: (1) District 5: City Park, Lakeshore/Lake Vista, Lakeview, and West End; (2) District 6: Filmore, Lake Terrace & Lake Oaks, Milenburg, Pontchartrain Park, and St. Anthony; and (3) District 9: Little Woods and Pines Village.

System Components and Data

Data used in this study were collected by the jointly operated U.S. Army Corps of Engineers (USACE)/U.S. Naval

Oceanographic Office (NAVO), Compact Hydrographic Airborne Rapid Total Survey (CHARTS) system. The CHARTS system is a unique sensor suite featuring an Optech's Scanning Hydrographic Operational Airborne LIDAR Survey (SHOALS)-3000T20, with a 3-kHz bathymetric LIDAR and a 20-kHz topographic LIDAR, an Itres CASI-1500 for hyperspectral imaging, and a DuncanTech-4000 digital camera (Wozencraft and Lillycrop, 2006). It has been utilized in many posthurricane surveys, including hurricanes Katrina and more recently Gustav and Ike, making it an ideal system to demonstrate the techniques used in this study (Macon, 2009; Macon, Wozencraft. and Broussard, 2008). From this integrated, airborne sensor suite, topographic and bathymetric LIDAR and aerial and hyperspectral imagery are further processed into an assortment of geographic information systems (GIS) data products for the National Coastal Mapping Program (NCMP), executed by the Joint Airborne LIDAR Bathymetry Technical Center of eXpertise (JALBTCX). These include 1-m seamless topo/bathy DEMs, 1-m bare-earth DEMs, true color orthorectified aerial image mosaics, postprocessed hyperspectral image mosaics, basic land-cover classifications, and zero-contour shoreline vectors (Macon, 2009; Wozencraft and Lillycrop, 2006; Wozencraft, Macon, and Lillycrop, 2007).

For this study, only topographic LIDAR, orthorectified aerial images and hyperspectral data were acquired because of insufficient water clarity needed for bathymetric LIDAR. The three individual surveys were collected approximately 1 year apart to alleviate major seasonal variations among the data sets on the following dates: (1) October 12 to December 12, 2005; (2) September 29 to October 4, 2006; and (3) November 7 to 20, 2007. All data were collected on a common platform, sharing an inertial navigation system and subject to common environmental effects (Macon, 2009). Generally, all three surveys were flown at 1000-m altitude with a 1-m spot spacing for the topographic LIDAR (± 15-cm elevation accuracy), collecting values for the first and last pulse returns in a single wavelength of light at 1064 nm. The hyperspectral imagery was collected at 1-m spatial resolution, including 36 spectral bands with 18-nm bandwidth in the 380- to 1050-nm spectral range. The time of flights was limited to within 3 hours of solar noon and a maximum 10% cloud cover for optimal quality (Macon and Wozencraft, 2008).

Data Processing

The topographic LIDAR data collected for this study were first processed into georeferenced point data by adjusting for the movement and path of the aircraft with position and orientation (POS) data collected during the flight. The LIDAR point data were downloaded and processed using Optech's SHOALS Ground Control System (GCS) software and then edited with Interactive Visualization Systems (IVS) 3D Fledermaus 6.7 software in the Pure File Magic (PFM) data format (Macon and Wozencraft, 2008). In Fledermaus, the LIDAR point data were manually edited and exported to American Standard Code for Information Interchange (ASCII) and LASer (LAS) 1.0 file formats for product development. Although both formats are useable by many software vendors, ASCII is a text file format and LAS is a standardized binary file format that retains unique LIDAR information (ASPRS, 2003). The LAS files were classified with Bentley's Microstation V8 software for engineering and GIS design projects. Using Terramodeler and Terrascan V9 applications within Microstation, the LIDAR ground, or bare-earth points, were identified through filtering and spatial statistics techniques (Macon and Wozencraft, 2008). The topographic first-return point data sets and bare-earth data sets were imported into Applied Imagery's Quick Terrain Modeler 6.0.6 software where DEMs were created using a triangulated irregular network (TIN) method commonly used for representation of vector point data in digital terrain modeling. Digital elevation models were developed for all of the acquired topographic LIDAR data, resulting in three first-return DEMs and three bare-earth DEMs, one set for each year.

Data collected from the CASI-1500 were first radiometrically corrected by converting the raw digital numbers to at-sensor radiance values with a calibration technique in Itres' Radcorr software program (Macon, 2009; Wozencraft, Macon, and Lillycrop, 2007). Then, atmospheric corrections were made to produce reflectance images using the U.S. Naval Research Laboratory's Tafkaa6s model, which removes atmospheric effects of light passing from the sun to the image scene and then to the aircraft (Gao, Heidebrecht, and Goetz, 1993). This process was conducted in ITT Visual Information Solutions (ITT VIS) ENVI 4.5 software for remote-sensing analysis as a custom added extension. Using additional Itres processing, the 1-m imagery was geopositioned using the same POS data used in processing the LIDAR data and then were orthorectified and mosaicked (Macon and Wozencraft, 2008).

Land-Cover Classification

The postprocessed LIDAR and hyperspectral data were integrated in the ENVI 4.5 software environment to create a basic land-cover classification. The height above ground, or surface height, was derived from the topographic and bare-earth LIDAR DEMs and combined with 36 CASI spectral bands in a decision-tree classifier (Macon, 2009). A decision-tree classification technique was selected because it has been widely used for successful land-cover classification and has the advantage of being a simple and intuitive process (Friedl and Brodley, 1997; Pal and Mather, 2003). It is the standard classification technique used to generate all basic land-cover classification data products developed for the NCMP and is widely applicable across a broad range of geographic conditions. The following land-cover types, described in Table 1, were identified: unclassified/saturated, water, bare ground/roads, structures, low vegetation, medium vegetation, and tall vegetation. These classes are similar to those identified in the basic land-cover classification standard data product as developed for the NCMP. They reflect general land-cover types found in all areas of the coastal United States and were selected to support delineation of land cover for hydrologic modeling, which typically requires identification of permeable and impermeable surfaces. They also take

Table 1. *Land-cover class names and general descriptions.*

Land-Cover Class	Class Description
Unclassified/saturated	Includes "no data" pixels and saturated pixels (undiscerned bright image objects)
Water	Includes inland waterways (*i.e.,* canals) and major water bodies (*i.e.,* Lake Pontchartrain)
Bare ground/roads	Includes nonvegetation pixels with height <1 m
Structures	Includes nonvegetation pixels with height >1 m
Low vegetation	Includes vegetation pixels defined by NDVI value >0.3 and height <0.5 m (*i.e.,* grasses)
Medium vegetation	Includes vegetation pixels defined by NDVI value >0.3 and height 0.5 to 6 m (*i.e.,* small trees/shrubs)
Tall vegetation	Includes vegetation pixels defined by NDVI value >0.3 and height >6 m (*i.e.,* trees)

NDVI = normalized difference vegetation index.

advantage of the height differences between classes that are discriminated with the LIDAR elevation data (*e.g.,* low, medium, and tall vegetation). Although the basic land-cover classification was not specifically designed for this study, it has the advantage of being analyzed with broadly developed techniques and includes elements of both the structural and natural environments, which are commonly assessed after a disaster (Hansen *et al.*, 2007).

The classification routine involved a series of decisions that successively partitioned the data into each class (Figure 2) as defined in the decision-tree framework (Friedl and Brodley, 1997). In the decision-tree framework "no data" and saturated pixels with scaled reflectance values of 0 or less than −1000 were identified as unclassified/saturated. Saturated pixels were considered skewed and are the result of very bright image objects, such as building rooftops (Macon, 2009). These values occur during the conversion to reflectance in the atmospheric correction. The separation of land and water pixels was tested with two different methods. The first was a band ratio between a blue/green band (529 nm) and a near-infrared band (1003 nm) where the result was greater than 1 or less than 0. The second was a Normalized Difference Vegetation Index (NDVI) band ratio between a near-infrared band (738 nm) and a red band (624 nm). Pixel values less than −0.05 were classified as water, whereas the rest were classified as land. Although both land and water separation methods worked well, neither produced perfect results. Ultimately, the NDVI method was chosen because it could also be used to further separate the land class into vegetation *vs.* nonvegetation, resulting in one computation to produce multiple classes and thus reducing overall processing time. In addition, it is a broadly tested method often used to identify and measure vegetation (Tucker, 1979). The NDVI result was also used to separate pixels with values greater than 0.3 for the vegetation class, whereas the rest (nonvegetation) were split into two categories using the LIDAR-derived surface height information. A height threshold greater than 1 m was used to identify structures in the nonvegetation pixels, and the remaining nonstructure pixels were separated into a combined class of roads and bare ground. Finally, the vegetation pixels were refined into three categories using height thresholds: <0.5 m for short grasses (low vegetation), 0.5–6 m for shrubs and small trees (medium vegetation), and >6 m for tall trees (tall vegetation) (Macon, 2009). This classification was applied to the combined hyperspectral and LIDAR data within the study area, resulting in three basic land-cover classifications, one for each year. Figure 3 illustrates the general land-cover classifications for each year as described in Table 1 and Figure 2.

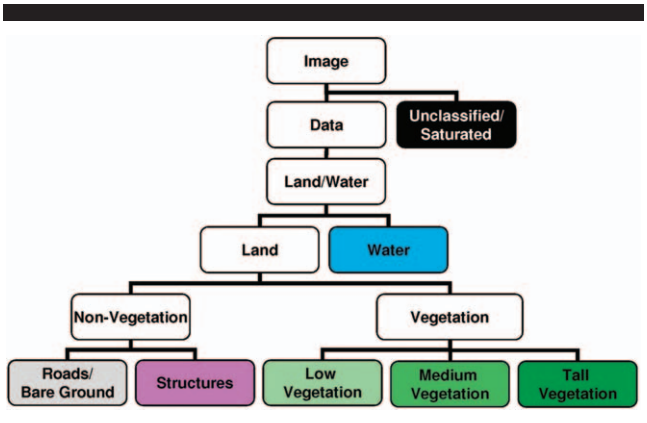

Figure 2. Illustration of the decision-tree classification process used to generate the land-cover classifications.

Change Detection

Change detection is a common technique in remote sensing used to identify and understand differences in earth objects

Figure 3. Land-cover classifications for the study area in 2005 (a), 2006 (b), and 2007 (c). Classes include unclassified/saturated (black), water (blue), bare grounds/roads (light grey), structures (pink), low vegetation (light green), medium vegetation (medium green), and tall vegetation (dark green). Note in (a) that much of the area is classified as bare grounds/roads because it was covered by mud and debris in the months after the disaster; many of these areas are classified as vegetation in (b) and (c). Also note the decrease in structures from (a) to (b) and (c), especially in neighborhoods like West End, Lakeview, Filmore (District 5), St. Anthony, Milneburg, Pontchartrain Park (District 6), Pines Village, and Little Woods (District 9).

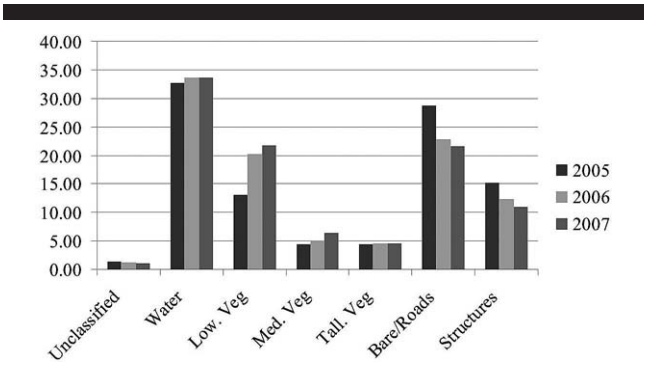

Figure 4. Land-cover class percentages by year.

over time due to changes in corresponding land cover for a wide variety of applications (Jensen and Im, 2007; Lu *et al.*, 2004; Singh, 1989). For this study, elevation and land-cover data for 3 years post-Katrina (2005, 2006, and 2007) were compared with a frequently used image-differencing technique (Jensen and Im, 2007; Lu *et al.*, 2004). First-return DEMs and basic land cover were differenced for each year to obtain corresponding difference data sets. For example, the 2006 first-return DEM was subtracted from the 2005 first-return DEM, and the 2007 first-return DEM was subtracted from the 2006 first-return DEM to identify annual changes in elevation and ultimately volume. Therefore, image differencing resulted in first-return elevation and land-cover changes from 2005 to 2006 and 2006 to 2007. Elevation difference images were analyzed to find both areas of erosion or loss and accretion or gain, with negative differences reflecting elevation loss and positive differences reflecting elevation gain. Only elevation changes greater than 1 m were identified to avoid changes that fall within the LIDAR accuracy margin or changes that may be associated with land subsidence, which was not the purpose of this study. Last, elevation changes were compared with land-cover changes through cross-tabulation to assess specific volume gains and losses within each land-cover class. All geospatial analyses were conducted in ENVI 4.5 and Environmental Systems Research Institute (ESRI) ArcGIS 9.2/9.3 software packages.

RESULTS

Overall land-cover percent changes by year are presented in Figure 4, and a detailed change detection matrix is displayed in Table 2. The top part of Table 2 shows the comparison between years 2005 and 2006; whereasthe bottom part shows the comparison between years 2006 and 2007. Total estimated volume changes are displayed in Table 3 and detailed volume changes by land-cover class are presented in Figure 5. Volume trends by land-cover class were calculated by cross-tabulating elevation changes for 2005 to 2006 with the 2005 land-cover classification (Figure 5a), and cross-tabulating elevation changes for 2006 to 2007 with the 2006 land-cover classification (Figure 5b). Total volume changes were derived from the first-return DEMs and were rounded to reflect approximate changes (Table 3). Volume changes by land-cover class were estimated from simplified, integer representations of the first-return DEMs due to algorithmic limitations for processing more complex floating point data (Figure 5). Unclassified/saturated and water classes were omitted from Figure 5 as they did not experience notable volume changes.

Land-Cover Changes

Table 2 and Figure 4 summarize the land-cover changes for 2005 to 2006 and 2006 to 2007. The study area includes a portion of Lake Pontchartrain and inland waterways and

Table 2. *Land-cover change detection matrix showing percentage changes, 2005 to 2006 (top) and 2006 to 2007 (bottom).*

	Unclassified	Water	Low Veg.	Med Veg.	Tall Veg.	Bare Ground/Roads	Structures	Row Total
2006					2005			
Unclassified	40.16	0.60	0.13	0.18	0.04	0.85	1.41	100
Water	47.40	98.99	0.14	0.28	0.05	0.83	2.00	100
Low veg.	2.28	0.03	76.47	17.70	5.64	28.86	5.72	100
Med veg.	0.44	0.01	4.11	47.89	10.04	2.56	7.89	100
Tall veg.	0.13	0.00	0.40	12.80	75.78	0.18	3.62	100
Bare ground/roads	7.74	0.31	17.13	8.87	3.78	63.82	9.88	100
Structures	1.85	0.06	1.63	12.27	4.67	2.91	69.49	100
Class total	100.00	100.00	100.00	100.00	100.00	100.00	100.00	0
Class changes	59.84	1.01	23.53	52.12	24.22	36.18	30.52	0
Image difference	−8.49	2.67	55.10	13.10	3.23	−20.54	−18.27	0
2007					2006			
Unclassified	42.29	0.63	0.18	0.19	0.04	0.43	1.47	100
Water	33.70	97.72	0.07	0.13	0.03	1.14	0.69	100
Low veg.	2.36	0.07	78.27	22.75	3.84	16.82	5.06	100
Med veg.	0.87	0.10	8.28	51.87	11.38	2.81	7.50	100
Tall veg.	0.18	0.01	0.28	10.26	81.44	0.12	2.01	100
Bare ground/roads	12.57	0.63	12.08	6.69	1.30	75.64	8.51	100
Structures	8.03	0.85	0.84	8.11	1.98	3.02	74.75	100
Class total	100.00	100.00	100.00	100.00	100.00	100.00	100.00	0
Class changes	57.71	2.28	21.73	48.13	18.56	24.36	25.25	0
Image difference	−13.16	0.03	7.23	27.08	0.06	−5.72	−11.14	0

Table 3. *Total volume loss and gains for the 34-km² study area. Values have been rounded and reflect approximate amounts.*

	2005–2006 Loss	2005–2006 Gain	Net Change	2006–2007 Loss	2006–2007 Gain	Net Change
Volume (m^3)	-8.1×10^6	$+6.5 \times 10^6$	-1.6×10^6	-7.2×10^6	$+5.1 \times 10^6$	-2.1×10^6
% Volume	−25.97	+20.75	−5.22	−26.71	+18.79	−7.92

canals, making up about 33% of the study area. Because the 2005 imagery was acquired well after the floodwaters receded, the land-cover classification includes assumed normal water levels for this time of year. In general, Figure 4 and Table 2 show that the areas of the vegetation classes increased, whereas the areas of the bare ground/roads and structures classes decreased. More specifically, bare ground/roads had a 21% decrease in 2006 compared with the original area in 2005 and a smaller decrease (6%) in 2007. This phenomenon is also illustrated in Figure 3, which shows that much of the area in 2005 was classified as bare ground/roads. This is because much of the area was covered by debris, mud, and other earthen material, especially in neighborhoods like West End and Lakeview (Figure 1) near the site of the 17th Street Canal breach. As recovery took place, the bare ground/roads class was replaced by other classes in 2006 and 2007, Table 2. The majority of this class changed to vegetation classes, especially low vegetation, 29% in 2006 and 17% in 2007.

Consequently, the decrease in the bare ground/roads class was also the reason for the corresponding increase in the vegetation classes. Low vegetation experienced a 55% area increase in 2006 compared with the original area in 2005 and another area increase of 7% in 2007 (Table 2). Medium and tall vegetation also experienced combined area increases of about 13% in 2006 as compared with their original respective areas in 2005. Medium vegetation experienced a 27% area increase in 2007, whereas tall vegetation area remained stable (Table 2). It was noted earlier that there was considerable damage and loss of forest and other vegetation after the disaster (FIA, 2005; Oswalt and Oswalt, 2008; Rodgers, Murrah, and Cooke, 2009; Wang and Xu, 2009; Wang *et al.*, 2010). In this case, one might expect a decrease in vegetation area. However, damage causes alterations to vegetation that may be the reason for the exchange among all of the vegetation classes during the classification and change detection. Other postdisaster debris analyses have shown that vegetation can move from its original location, changing the structural components and quantities. In addition, there can be confusion between debris types that lead to overestimation of vegetation debris that should be classified as structural debris (Hansen *et al.*, 2007).

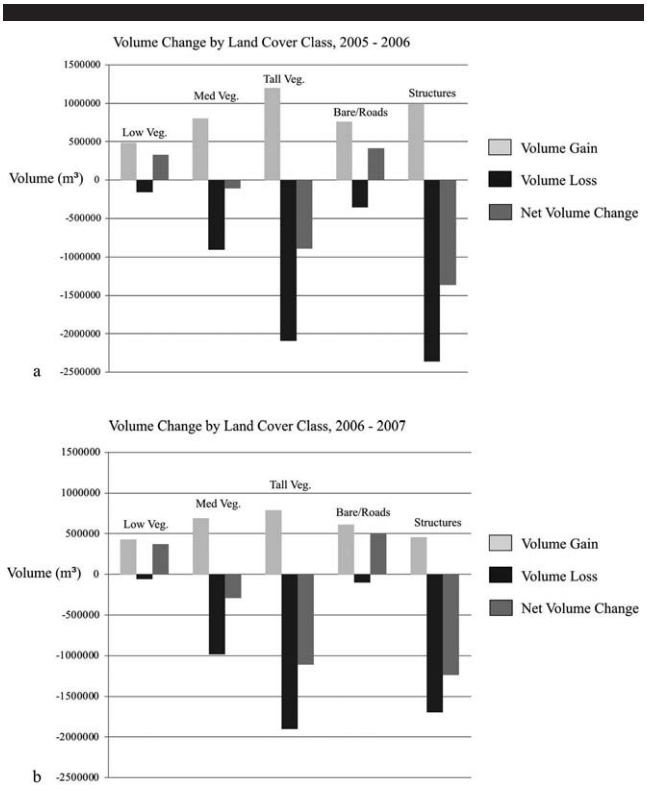

Figure 5. Estimated volume loss and gain by land-cover class for 2005–2006 (a) and 2006–2007 (b).

Because much of the area was covered by earthen material and classified as bare ground/roads in 2005 and was eventually cleared, much of the low vegetation was presumably covered and not classified as vegetation. Therefore, in 2006 there was a fairly large area increase in low vegetation (55%), mostly gained from the bare ground/roads class. Other major contributions to the low vegetation class were from the medium and tall vegetation classes. Assuming damage to or clearing of the taller-elevation vegetation classes, this exchange also helps explain the area increase in low vegetation. Smaller area contributions to the low vegetation class (5 to 6%) were also seen from the structures class. Most of the area increase to medium vegetation came from the other vegetation classes and some from the structures class. Notable increases in the medium-vegetation class for the 2 years (13 and 27%) were primarily the result of damages associated with the tall-vegetation and structures class. Other gains to the medium-vegetation class came from the low-vegetation class (4 and 8%) and could be assumed normal vegetation growth, as well as some compositional or structural changes resulting from damage. It is worth noting that some changes between vegetation classes may be the result of minor seasonal variations between surveys. Although the surveys were generally conducted at the same time of year, spanning the months between September and December, minor seasonal differences are expected and could account for some of the change between the various vegetation classes.

The structures class had area decreases in 2005 to 2006 and 2006 to 2007 (18 and 11%, respectively). The widespread damage to buildings across the study area explains this

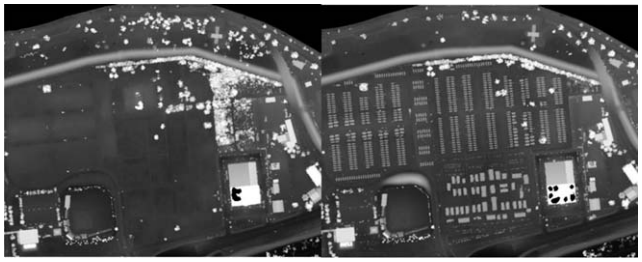

Figure 6. Example of first-return DEMs from 2005 (left) and 2006 (right) for an area in the eastern part of the Lake Terrace and Oaks neighborhood. The 2006 image shows a temporary housing development and loss of vegetation after the disaster.

decrease, as a large number of demolitions and structural remodeling followed the disaster, especially in the first year. It is worth noting that there was some confusion in the land-cover classification, especially in the water category. For example, changes in the structures class show that some of these areas were replaced by water, which is not likely. Visual inspections of the land-cover classifications show that some pixels near buildings were classified as water, although they were likely shadows that were misclassified.

Volume Changes

Estimated volume changes included a net volume decrease of 1.6×10^6 m^3 in 2005 to 2006 and a net volume decrease of 2.1×10^6 m^3 in 2006 to 2007 (Table 3). The changes in volume illustrate some of the major physical impacts of the disaster and ensuing recovery period. To put these numbers into context with other post-Katrina assessments, a report from the U.S. Geological Survey (USGS) is used (Hansen *et al.*, 2007). This report includes a summary of estimated debris volumes after hurricane Katrina using topographic LIDAR and high-resolution aerial imagery. Imagery classifications identified vegetation and nonvegetation (structural) debris in a heavily damaged, 24-km^2 study area along the Mississippi coast. The report estimated a total of approximately 3.4×10^6 m^3 of vegetation debris and 5.6×10^6 m^3 of nonvegetation debris (Hansen *et al.*, 2007). The numbers from this report further illustrate the unprecedented and billions of dollars worth of damage across the region, and additionally illustrate the scope of damage and subsequent recovery in the study area.

Figure 5 presents estimated volume changes by land-cover class for 2005 to 2006 (a) and 2006 to 2007 (b). In general, low-vegetation and bare ground/roads classes had net volume increases, whereas medium- and tall-vegetation and structures classes had net volume decreases during this time period. Although the bare ground/roads class had area decreases (Table 2), Figure 5 shows that this class had net volume increases. Since most of the land-cover change in the bare ground/roads class was to the low-vegetation class, most of the elevation increase was small, however extensive (28% of the bare ground/roads class, 2005 to 2006). Furthermore, changes in the bare ground/roads class included land-cover changes to medium vegetation and structures, which also contributed to the net volume increase. An example of this can be seen in Figure 6, which shows elevation changes in the eastern part of the Lake Terrace & Oaks neighborhood (Figure 1). This figure shows a new temporary housing development that appeared after hurricane Katrina in 2006. Low vegetation also had net volume increases for this time period (Figure 5). Much of the land-cover change in the low-vegetation class was to the bare ground/roads class (17 and 12%), again assuming that elevation and volume increases were small, though extensive. However, some land-cover changes to medium vegetation (4 and 8%) were enough to result in a net volume increase in low vegetation, especially in 2006 to 2007.

Other classes, such as medium and tall vegetation, had net volume decreases during this time period. Although the overall percentage of medium vegetation looks fairly stable with a slight increase (Figure 4), there were quite a few changes within the class (Table 2). This table shows that much of the land-cover change within this class was to lower-elevation classes, such as low vegetation (18 and 23%) and bare ground/roads (9 and 7%), accounting for the net decrease in volume, which was not enough to offset elevation gains in land-cover changes to tall vegetation or structures (Figure 5). Similarly, land-cover changes within the tall-vegetation class were to lower-elevation classes, especially medium vegetation (Table 2), and resulted in net volume decreases (Figure 5). Presumably, damage and loss of vegetation along with structural and compositional changes caused much of the net volume decrease after hurricane Katrina. To put the damage into context, the findings in our study were compared with those produced by the U.S. Department of Agriculture (USDA) Forest Service, Forest Inventory and Analysis (FIA, 2005). They found that 45% of the affected timberland in Louisiana was damaged, with potential total timber loss volumes estimated at approximately 25×10^6 m^3. Totaling the net volume decreases (2005 to 2006 and 2006 to 2007) for both medium- and tall-vegetation classes (2.4×10^6 m^3), our findings represent about 10% of that total potential volume loss in Louisiana. Although vegetation is likely defined differently in both studies, the USDA provides one of the few published estimates for comparison and it is only meant to provide a general context.

Last, the structures class also had net volume decreases as expected during this time period (Figure 5). Changes to existing structures were reflected in the net volume decrease due to the damage and subsequent demolition of many structures, which is why this class changed to lower-elevation classes. To provide a context for the amount of structural volume loss, a comparison was made using data from the New Orleans City Planning Commission (City of New Orleans, 2006). Unfortunately, the number of structures in our study area was not known; however, using the number of lots, we estimated the number of structures. The planning commission defines a lot as a parcel of land that may be occupied by a building. Lots for the area covering Orleans Parish were available in our study area (a little over half the study area), whereas the number of lots in Jefferson Parish was unknown. The estimated number of lots was 10,000 for the Orleans

Parish portion of the study area, including many large land parcels with multiple buildings (*e.g.,* The University of New Orleans in the Lake Terrace & Oaks neighborhood, Figure 1). Therefore, we doubled the number of lots to account for structures in Jefferson Parish and those on large lots to get an approximate number of 20,000 structures in our study area before the disaster. Since many of the structures in our study area were residences, we approximated the average structural volume at 555 m^3 (3-m elevation $\times$ 185-m^2). Therefore, the total estimated structural volume before the disaster is estimated at 11 $\times$ 10^6 m^3 (20,000 structures $\times$ 555 m^3). Totaling the net volume decreases (2005 to 2006 and 2006 to 2007) for the structures class (2.6 $\times 10^6$ m^3), our findings represent about 23% of that estimated structural volume loss. This is not surprising considering the structural devastation in neighborhoods like West End and Lakeview (Figure 1).

DISCUSSION

This study achieved the goal of utilizing imagery collected by an integrated sensor suite, CHARTS, to illustrate how image fusion of hyperspectral and LIDAR data can be used to assess physical changes and recovery along the south shore of Lake Pontchartrain, Louisiana in response to hurricane Katrina. It demonstrates an innovative use for hyperspectral and LIDAR fusion to assess postdisaster recovery and presents broadly applicable methods that can be used in any coastal environment. It also provides impetus for the future use of remote-sensing technology beyond the initial response phase into the longer-term recovery phase of the disaster management cycle. This study included data for 3 years after the disaster, and it illustrated that physical changes to structures and vegetation continue long after the event, further demonstrating the need for geospatial assessment in the recovery phase.

One advantage of using a sensor suite such as CHARTS is that all of the sensors are tied to the same navigation system on a common platform, alleviating coregistration problems and errors that often plague attempts to combine multiple data sources. In disaster response mapping, this is especially true when examining fine-scale damage and change, such as to individual structures or vegetation. Damage estimates derived from these assessments are crucial for recovery, and studies such as this can be used to assist in that process. Traditionally, reports such as the Brookings Institution Metropolitan Policy Program & Greater New Orleans Community Data Center (2009) are used to track recovery after an event like Hurricane Katrina. The report provides valuable information related to rebuilding, blight, residual flood risk, repopulation, and other statistics. However, the report acknowledges that tracking recovery is challenging and that no standardized indicators, such as for land loss, restoration, and mitigation, exist (Brookings Institution, 2009). This study demonstrates the capability and methods to provide detailed structural and vegetation information that can be used in part to address coastal indicators, assisting with the challenge of assessing recovery. The results of this study complement the findings in the Brookings Institution 2009 report; they provide more detailed information within overall trends identified in the report, such as the decrease in housing structures and net gain in empty lots, illustrating how they can be used together to learn even more about recovery.

The results and methods from this study can also be useful in the coastal planning process. Large-scale impacts continue long after the disaster and remote-sensing analyses, such as the one presented in this study, provide the advantage of assessing changes over a wide geographic area while also providing high-resolution data. Furthermore, the additional capability of fusing hyperspectral and LIDAR data provides simultaneous qualitative and quantitative information that currently cannot be replicated on such an order of detail with any single-sensor system. This advantage can have important implications for addressing coastal planning and resiliency. For example, the methods and results determined in this study could be used to help target funding for development or restoration initiatives, identify habitats or habitat configurations that are more vulnerable or robust in environmental planning alternatives, and examine the vulnerability of coastal structures in terms of geographic location. In addition, this information could be used to address changes in zoning and prioritizing recovery assistance and other patterns that might not be apparent at a district or neighborhood level.

Whatever advantages this approach may provide in the planning process, there are still major challenges with assessing long-term recovery and integrating remote-sensing analyses and other studies into the coastal planning process. The CHARTS system continually collects data in the study area and annual changes will continue to be analyzed to improve the described methods. New efforts for better comparison of elevation, volumetric, and land-cover class data are being considered, as well as better feature extraction tools for assessing structural features as possible improvements to this study. Other improvements to this study include ground truthing and accuracy assessments for the land-cover classification, DEMs, and the results of the change detection, which would greatly enhance the results and findings. Also, the lack of data characterizing conditions immediately before Katrina made landfall meant there was no baseline data set for comparison, which is critical for comparing long-term recovery and trends.

CONCLUSIONS

The use of remote-sensing technologies for posthurricane disaster response and assessment has increased considerably over the last decade as systems continue to advance and vulnerable coastal areas continue to face disaster. This study provides an example of a postdisaster recovery assessment through the analysis of coastal land-cover, elevation, and volume changes over a 3-year period after Hurricane Katrina. It provides clues and information regarding damage and initial recovery trends that are important for coastal planning and management decision making. It also presents innovative methods for integrating different data sources, such as hyperspectral and LIDAR data, to extract detailed and unique land-cover and elevation information. This combination of resources also provides new ways of examining

changes resulting from a natural disaster and learning more about recovery in the landscape.

Some have noted the lack of geographic analyses in the recovery phase of the disaster management cycle (Hill *et al.*, 2006; Ward, Leitner, and Pine, 2010), and this study attempts to address that research gap by providing an important first step, using advanced remote-sensing technology and imagery resources to assess recovery. It also complements other initial attempts to address post-Katrina recovery trends, such as those presented by Ward, Leitner, and Pine (2010), in which a spatial assessment of recovery was conducted by combining social and physical parameters in a modeling framework. This study developed a spatial recovery index for New Orleans and illustrates a generalized geographic recovery pattern, confirming variable recovery rates throughout the city at the neighborhood or broader level. Our study provides a finer scale of analysis and can be used to gain further insight into the recovery process. Newer remote-sensing processing techniques, such as the fusion of hyperspectral imagery and LIDAR data, as well as other spatial approaches, can provide innovative solutions and critical information for coastal planning. However, challenges remain for better integration of studies such as these into the coastal planning process, and ultimately for improved coastal resiliency.

ACKNOWLEDGMENTS

The projects, analysis, and resulting data described herein, unless otherwise noted, were obtained from work performed by the JALBTCX and funded by USACE Headquarters and the System-Wide Water Resources Program (SWWRP). The use of trade names does not constitute an endorsement in the use of these products by the U.S. Government. Permission was granted by the Chief of Engineers to publish this work.

LITERATURE CITED

ASPRS (American Society for Photogrammetry and Remote Sensing), 2003. *Superseded ASPRS LIDAR Data Exchange Format Standard Version 1.0*. American Society for Photogrammetry and Remote Sensing (ASPRS) Standards Committee, 9p. http://www.asprs.org/society/committees/standards/asprs_las_format_v10.pdf (accessed February 24, 2010).

Barnes, C.F.; Fritz, H., and Yoo, J., 2007. Hurricane disaster assessments with image-driven data mining in high-resolution satellite imagery. *IEEE Transactions on Geoscience and Remote Sensing,* 45(6), 1631–1640.

Barras, J.A., 2006. Land Area Change in Coastal Louisiana after the 2005 Hurricanes—A Series of Three Maps: U.S. Geological Survey Open-File Report 2006-1274.

Barras, J.A., 2007. Land area changes in coastal Louisiana after Hurricanes Katrina and Rita. *In:* Farris, G.S.; Smith, G.J.; Crane, M.P.; Demas, C.R.; Robbins, L.L., and Lavoie, D.L. (eds.), *Science and Storms—the USGS Response to the Hurricanes of 2005: U.S. Geological Survey Circular 1306,* p.98–113.

Barras, J.A., 2009. Land area change and overview of major hurricane impacts in coastal Louisiana, 2004–08: U.S. Geological Survey Scientific Investigations Map 3080, 6p.

Brookings Institution Metropolitan Policy Program & Greater New Orleans Community Data Center, 2009. *The New Orleans Index: Tracking the Recovery of New Orleans & the Metro Area*. Washington, DC: Brookings Institution, August 2009.

Chust, G.; Galparsoro, I.; Borja, A.; Franco, J., and Uriarte, A., 2008. Coastal and estuarine habitat mapping, using LIDAR height and intensity and multi-spectral imagery. *Estuarine, Coastal and Shelf Science,* 78(1), 633–643.

City of New Orleans, 2006. City of New Orleans Geographic Information Systems (CNOGIS), New Orleans City Planning Commission, GIS Data Portal. http://gisweb.cityofno.com/cnogis/dataportal.aspx (accessed February 24, 2010.)

Elaksher, A., 2008. Fusion of hyperspectral images and LIDAR-based DEMs for coastal mapping. *Optics and Lasers in Engineering,* 46(7), 493–498.

Fearnley, S.M.; Miner, M.D.; Kulp, M.; Bohling, C., and Penland, S., 2009. Hurricane impact and recovery shoreline change analysis of the Chandeleur Islands, Louisiana, USA: 1855–2005. *Geo-Marine Letters,* 29(6), 455–466.

FIA (Forest Inventory and Analysis), 2005. Potential Timber Damage Due to Hurricane Katrina in Mississippi, Alabama, and Louisiana, September 22, 2005. Forest Inventory and Analysis, Southern Research Station. http://www.srs.fs.usda.gov/katrina/katrina_brief_2005-09-22.pdf (accessed February 24, 2010).

Friedl, M.A. and Brodley, C.E., 1997. Decision tree classification of land cover from remotely sensed data. *Remote Sensing of Environment,* 61(3), 399–406.

Friedland, C.J.; Levitan, M.L., and Adams, B.J., 2008. Suitability of remote sensing per-building damage assessment of residential buildings subjected to hurricane storm damage. *Proceedings of the 6th International Workshop on Remote Sensing for Disaster Applications* (Pavia, Italy, European Centre for Training and Research in Earthquake Engineering).

Fritz, H.M.; Blount, C.; Sokoloski, R.; Singleton, J.; Fuggle, A.; McAdoo, B.; Moore, A.; Grass, C., and Tate, B., 2007. Hurricane Katrina storm surge distribution and field observations on the Mississippi Barrier Islands. *Estuarine, Coastal and Shelf Science,* 74(1–2), 12–20.

Froede, C.R., Jr., 2008. Changes to Dauphin Island, Alabama, brought about by Hurricane Katrina (August 29, 2005). *Journal of Coastal Research,* 24(3), 110–117.

Gao, B.C.; Heidebrecht, K.B., and Goetz, A.F.H., 1993. Derivation of scaled surface reflectances from AVIRIS data. *Remote Sensing of Environment,* 44(2–3), 165–178.

Geerling, G.W.; Labrador-Garcia, M.; Clevers, J.G.P.W.; Ragas, A.M., and Smits, A.J.M., 2007. Classification of floodplain vegetation by data fusion of spectral (CASI) and LIDAR data. *International Journal of Remote Sensing*. 28(19), 4263–4284.

Ghosh, S.; Adams, B.J.; Womble, J.A.; Friedland, C., and Eguchi, T., 2007. Deployment of remote sensing technology for multi-hazard post-Katrina damage assessment. *Proceedings of the 2nd International Conference on Urban Disaster Reduction* (Taipei, Taiwan).

Hansen, M.; Howd, P.; Sallenger, A.; Write, W, and Lillycrop, J., 2007. Estimation of post-Katrina debris volume: an example from coastal Mississippi. *In:* Farris, G.S.; Smith, G.J.; Crane, M.P.; Demas, C.R.; Robbins, L.L., and Lavoie, D.L. (eds.), *Science and Storms—the USGS Response to the Hurricanes of 2005: U.S. Geological Survey Circular 1306,* pp. 43–48.

Hill, A.A.; Keys-Mattews, L.D.; Adams, B.J., and Podolsky, D., 2006. Remote Sensing and Recovery: A Case Study on the Gulf Coast of the United States. *Proceedings of the 4th International Workshop on Remote Sensing for Disaster Response* (Cambridge, United Kingdom).

Hill, R.A. and Thompson, A.G., 2005. Mapping woodland species composition and structure using airborne spectral and LIDAR data. *International Journal of Remote Sensing*. 26(17), 3763–3779.

Jensen, J.R. and Im, J., 2007. Remote sensing change detection in urban environments. *In:* Jensen, J.R.; Gatrell, J.D., and McLean, D. (eds.), *Geo-Spatial Technologies in Urban Environments*. Berlin: Springer, pp. 7–31.

Klemas, V.V., 2009. Remote sensing of coastal resources and environment. *Environmental Research, Engineering and Management,* 48(2), 11–18.

Knabb, R. D.; Rhome, J.R., and Brown, D.P., 2005. Tropical Cyclone Report: Hurricane Katrina, 23–30 August 2005. Miami, Florida: National Oceanic and Atmospheric Administration, National Hurricane Center, 43p.

Lefsky, M.A.; Cohen, W.B.; Parker, G.G., and Harding, D.J., 2002.

LIDAR remote sensing for ecosystem studies. *Bioscience,* 52(1), 19–30.

Lillesand, T.M.; Kiefer, R.W., and Chipman, J.W., 2008. *Remote Sensing and Image Interpretation*, 6th edition. Hoboken, New Jersey: John Wiley & Sons, 804p.

Lu, D.; Mausel, P.; Brondizio, E., and Moran, E., 2004. Change detection techniques. *International Journal of Remote Sensing,* 25(12), 2365–2401.

Macon, C.L., 2009. USACE National Coastal Mapping Program and the Next Generation of Data Products. *Proceedings of the OCEANS 2009 MTS/IEEE Biloxi Conference* (Biloxi, Mississippi).

Macon, C.L. and Wozencraft, J.M., 2008. Regional land cover classifications using topographic LIDAR and hyperspectral imagery. *Proceedings of the 8th Annual International LIDAR Mapping Forum* (Denver, Colorado).

Macon, C.L.; Wozencraft, J.L., and Broussard, C.N., 2008. New Orleans area topographical and hyperspectral changes over the past 3 years. *Proceedings of the 2008 PIANC Gulf Coast Hurricane Conference* (Mobile, Alabama).

Mundt, J.T.; Streutker, D.R., and Glenn, N.F., 2006. Mapping sagebrush distribution using fusion of hyperspectral and LIDAR classifications. *Photogrammetric Engineering & Remote Sensing,* 72(1), 47–54.

NOAA (National Oceanic and Atmospheric Administration), 2006. Land Cover Data for Hurricane Katrina Impacted Areas, Katrina Land Cover Change Data. National Oceanic and Atmospheric Administration, Coastal Services Center, Coastal Change Analysis Program (C-CAP). http://www.csc.noaa.gov/crs/lca/katrina/ (accessed January 15, 2010).

NOAA, 2008. LIDAR 101: An Introduction LIDAR Technology, Data, and Applications. National Oceanic and Atmospheric Administration, Coastal Services Center, Coastal Geospatial Services Division, Coastal Remote Sensing Program. http://csc.noaa.gov/digitalcoast//data/coastallidar/What_is_Lidar.pdf (accessed February 24, 2010).

Oswalt, S.N. and Oswalt, C.M., 2008. Relationships between common forest metrics and realized impacts of Hurricane Katrina on forest resources in Mississippi. *Forest Ecology and Management,* 255(5–6), 1692–1700.

Pal, M. and Mather, P.M., 2003. An assessment of the effectiveness of decision tree methods for land cover classification. *Remote Sensing of Environment,* 86(4), 554–565.

Rodgers, J.C.; Murrah, A.W., and Cooke, W.H., 2009. The impact of Hurricane Katrina on the coastal vegetation of the Weeks Bay Reserve, Alabama from NDVI data. *Estuaries and Coasts,* 32(3), 496–507.

Singh, A., 1989. Digital change detection techniques using remotely sensed data. *International Journal of Remote Sensing,* 10(6), 989–1003.

Smith, R.A.; Irish, J.L, and Smith, M.Q., 2000. Airborne LIDAR and airborne hyperspectral imagery: a fusion of two proven sensors for improved hydrographic surveying. *Proceedings of Canadian Hydrographic Conference* (Montreal, Canada).

Stoker, J.M.; Tyler, D.J.; Turnipseed, D.P.; Wilson, K.V., and Oimoen, M.J., 2009. Integrating disparate LIDAR data sets for a regional storm tide inundation analysis of Hurricane Katrina. *Journal of Coastal Research,* SI(53), 66–72.

Tucker, C.J., 1979. Red and photographic infrared linear combinations for monitoring vegetation. *Remote Sensing of the Environment,* 8, 127–150.

Vijayaraj, V.; Bright, E.A., and Bhaduri, B.L., 2008. Rapid damage assessment from high-resolution imagery. *Proceedings of the International Geoscience and Remote Sensing Symposium* (Boston, Massachusetts).

Wang, F. and Xu, Y.J., 2009. Hurricane Katrina-induced forest damage in relation to ecological factors at landscape scale. *Environmental Monitoring and Assessment,* 156(1–4), 491–507.

Wang, W.; Qu, J.J.; Hao, X.; Liu, Y., and Stanturf, J.A. 2010. Post-hurricane forest damage assessment using satellite remote sensing. *Agricultural and Forest Meteorology,* 150(1), 122–132.

Ward, S.M.; Leitner, M., and Pine, J., 2010. Investigating recovery patterns in postdisaster urban settings: utilizing geotechnology to understand post-Hurricane Katrina recovery in New Orleans, Louisiana. *In:* Showater, P.S. and Lu, Y. (eds.), *Geospatial Techniques in Urban Hazard and Disaster Analysis*. Dordrecht, The Netherlands: Springer, pp. 355–372.

Womble, J.A.; Ghosh, S.; Friedland, C.J., and Adams, B.J., 2006. *Hurricane Katrina—Advanced Damage Detection for Hurricane Katrina: Integrating Remote Sensing and VIEWS™ Field Reconnaissance*, Volume 2. MCEER-06-SP02, Buffalo, New York, 154p.

Womble, J.A.; Mehta, K.C, and Adams, B.J., 2008. Remote sensing of hurricane damage—part 1 toward automated damage assessment. *Proceedings of the American Association of Wind Engineers Workshop* (Vail, Colorado).

Wozencraft, J.M. and Lillycrop, W.J., 2006. JALBTCX coastal mapping for the USACE. *International Hydrographic Review,* 7(2), 28–37.

Wozencraft, J.M.; Macon, C.L., and Lillycrop, W.J., 2007. CHARTS-enabled data fusion for coastal zone characterization. *Proceedings of the Sixth International Symposium on Coastal Engineering and Science of Coastal Sediment Processes 2007* (Reston, Virginia, ASCE), pp. 1827–1836.